

# The central electrode correction factor for high-Z electrodes in small ionization chambers

B. R. Muir<sup>a)</sup> and D. W. O. Rogers<sup>b)</sup>

Ottawa Carleton Institute for Physics, Carleton University Campus, 1125 Colonel By Drive, Ottawa, Ontario K1S 5B6, Canada

(Received 20 September 2010; revised 10 November 2010; accepted for publication 7 December 2010; published 31 January 2011)

**Purpose:** Recent Monte Carlo calculations of beam quality conversion factors for ion chambers that use high-Z electrodes [B. R. Muir and D. W. O. Rogers, *Med. Phys.* **37**, 5939–5950 (2010)] have shown large deviations of  $k_Q$  values from values calculated using the same techniques as the TG-51 and TRS-398 protocols. This report investigates the central electrode correction factor,  $P_{cel}$ , for these chambers.

**Methods:** Ionization chambers are modeled and  $P_{cel}$  is calculated using the EGSnrc user code `egs_chamber` for three cases: in photon and electron beams under reference conditions; as a function of distance from an iridium-192 point source in a water phantom; and as a function of depth in a water phantom on which a 200 kVp x-ray source or 6 MV beam is incident.

**Results:** In photon beams, differences of up to 3% between  $P_{cel}$  calculations for a chamber with a high-Z electrode and those used by TG-51 for a 1 mm diameter aluminum electrode are observed. The central electrode correction factor for a given value of the beam quality specifier is different depending on the amount of filtration of the photon beam. However, in an unfiltered 6 MV beam,  $P_{cel}$  varies by only 0.3% for a chamber with a high-Z electrode as the depth is varied from 1 to 20 cm in water. The difference between  $P_{cel}$  calculations for chambers with high-Z electrodes and TG-51 values for a chamber with an aluminum electrode is up to 0.45% in electron beams. The central electrode correction, which is roughly proportional to the chambers absorbed dose sensitivity, is found to be large and variable as a function of distance for chambers with high-Z and aluminum electrodes in low-energy photon fields.

**Conclusions:** In this work, ionization chambers that employ high-Z electrodes have been shown to be problematic in various situations. For beam quality conversion factors, the ratio of  $P_{cel}$  in a beam quality  $Q$  to that in a Co-60 beam is required; for some chambers,  $k_Q$  is significantly different from current dosimetry protocol values because of central electrode effects. It would be best for manufacturers to avoid producing ion chambers that use high-Z electrodes. © 2011 American Association of Physicists in Medicine. [DOI: 10.1118/1.3532818]

Key words: central electrode factor,  $P_{cel}$ , ionization chambers, Monte Carlo, EGSnrc

## I. INTRODUCTION

The calibration of high-energy radiation sources is based on absorbed dose-to-water standards and the use of gas-filled ionization chambers. To ensure proper beam calibration, the use of clinical reference dosimetry protocols is required.<sup>1–3</sup> Increased adoption of radiation therapy techniques using small fields has provoked the advent of ionization chambers with much smaller volumes than standard Farmer-type chambers. Many of these ion chambers have electrodes composed of high-Z materials. These chambers are not characterized in dosimetry protocols except for two chambers in recent versions of the TRS-398 protocol.<sup>4</sup>

In a recent publication by Muir and Rogers,<sup>5</sup> direct Monte Carlo calculations of beam quality conversion factors,  $k_Q$ , are provided for 32 ion chambers. Of these, five chambers were simulated that employ high-Z central electrodes. For these chambers, it was noted that  $k_Q$  exhibits the largest deviation from TG-51-type calculations using central electrode correction factors for an aluminum electrode. The deviation is at-

tributed to the composition of the central electrode as Monte Carlo calculations of  $k_Q$  for the same chambers without a central electrode are in much better agreement with TG-51-type calculations.<sup>5</sup> McEwen<sup>6</sup> determined experimental  $k_Q$  factors for 27 ion chambers, including 3 chambers with high-Z electrodes. Among all chambers in this study, two of these, the Exradin A16 and the IBA CC01, demonstrate the largest maximum deviation from  $k_Q$  values calculated using TG-51-like methods. It was noted that they also show unexpected recombination behavior and large polarity corrections. In the past, studies of central electrode correction factors have focused on ion chambers with aluminum or graphite electrodes,<sup>7–11</sup> although other investigations have reported strange behavior with ion chambers using high-Z electrodes.<sup>12–15</sup>

Considering the abundance of publications indicating issues with ion chambers that employ high-Z electrodes, there is motivation for a complete study on the effect of the central electrode for these chambers. This work presents a Monte

TABLE I. Specifications of the ionization chamber models. The materials are air equivalent plastic (C552), tissue equivalent plastic (A150), silver-plated copper covered steel (SPC), polymethylmethacrylate (PMMA), graphite (Gr), and aluminum (Al). The nominal volume,  $V$ , is given in the first column; in some cases, this is different from the active volume calculated using chamber specifications.

Chamber (V/cm <sup>3</sup> )	Wall		Electrode			Active cavity	
	Material	Thickness (mm)	Material	Radius (mm)	Length (mm)	Radius (mm)	Length (mm)
<b>Exradin</b>							
A12 (0.65)	C552	0.5	C552	0.5	21.6	3.05	24.8
A14 (0.016)	C552	1.0	SPC	0.165	1.5	2.0	2.0
T14 (0.016)	A150	1.0	SPC	0.165	1.5	2.0	2.0
A14SL (0.016)	C552	1.1	SPC	0.165	1.5	2.025	2.0
A16 (0.007)	C552	0.5	SPC	0.165	1.3	1.2	2.4
<b>PTW</b>							
31010 (0.125)	PMMA/Gr	0.55/0.15	Al	0.55	6.0	2.75	6.5
31006 (0.015)	PMMA/Gr	0.57/0.09	Steel	0.09	4.0	1.0	5.0
31014 (0.015)	PMMA/Gr	0.57/0.09	Al	0.09	4.0	1.0	5.0
<b>IBA</b>							
CC01 (0.01)	C552	0.5	Steel	0.175	2.7	1.0	3.6
<b>NE</b>							
NE2571 (0.6)	Gr	0.36	Al	0.5	20.5	3.14	24.0
NE2561 (0.3)	Gr	0.53	Al	1.0 <sup>a</sup>	6.5	3.7	9.0

<sup>a</sup>The NE2561 has a hollow electrode with a 0.2 mm thick aluminum shell. The air inside the aluminum layer is not considered part of the active cavity.

Carlo investigation of the central electrode correction factor,  $P_{cel}$ , which is defined as the ratio of the dose to the gas in an ion chamber without the central electrode ( $D_{ch}$ ) to that with the central electrode ( $D_{ch}^{el}$ ),

$$P_{cel} = \frac{D_{ch}}{D_{ch}^{el}}. \quad (1)$$

## II. METHODS

The `egs_chamber` user code of Wulff *et al.*<sup>16</sup> for the EGSnrc Monte Carlo code system<sup>17</sup> is used to maximize simulation efficiency. The `egs++` geometry package is used to model construction details of the ion chambers simulated here. Chamber models are derived from manufacturer blueprints for the Exradin and the IBA CC01 ion chambers and from manufacturers' user manuals for all other chambers. Correlated sampling in `egs_chamber` is used to calculate  $P_{cel}$  using Eq. (1). Chambers simulated here include the Exradin A16, T14, A14, and A14SL; the IBA CC01; the NE2561; and the PTW 31010, 31006, and 31014 chambers. Additionally, two standard Farmer-type chambers, the NE2571 and Exradin A12, are studied for comparison to calculations with small-volume chambers. Chamber specifications are given in Table I. Since specifications and materials from Exradin blueprints are proprietary, the data in Table I for these chambers are taken from the user manual, although for calculations, the blueprint specifications are used. The ion chamber models used here are the same as in our previous study,<sup>5</sup> except for the NE2561. More realistic specifications were

obtained for the NE2561 (M. McEwen, 2010, private communication). Calculations of  $P_{cel}$  are performed with the chamber at the reference depth on the central axis of the beam in a  $30 \times 30 \times 30$  cm<sup>3</sup> water phantom for the chambers in Table I.

Calculations of  $P_{cel}$  in this work differ from other publications in that the chamber stem is included in these calculations. The dose to the gas without the central electrode is calculated by changing the central electrode in the stem to the material adjacent to the electrode and the central electrode in the active region to air. However, calculations of  $P_{cel}$  for the NE2571 agree with those of Buckley *et al.*<sup>11</sup> where no stem is considered. Calculations using the classical method (without a stem) and the method used here for the A16 and CC01 chambers exhibit a maximum difference of only 0.25%. The definition of  $P_{cel}$  used here takes into account most of the non-negligible effects on the absorbed dose-to-air introduced by the presence of high-Z materials in the stem as well as in the cavity.

In photon beams, the reference depth is taken to be 5 cm for a cobalt-60 source and 10 cm for all other sources. Sources are modeled from photon spectra using a point source collimated to a  $10 \times 10$  cm<sup>2</sup> field on the surface of the phantom at an SSD of 100 cm. Calculations of  $P_{cel}$  for the Exradin A16 chamber were also performed using a full BEAMnrc model as the source for the <sup>60</sup>Co unit and the Elekta SL25 6 MV and Varian 18 MV linear accelerators. Negligible differences between calculations performed with a point source were observed compared to the relative uncer-

TABLE II. Radiation sources and beam quality specifiers. For photon beams, beam quality is specified by the photon component of the percent depth-dose at 10 cm for a  $10 \times 10$  cm<sup>2</sup> field on the surface of the water phantom,  $\%dd(10)_x$ . For electron beams, the beam quality specifier is  $R_{50}$ , the depth in water at which the absorbed dose falls to 50% of the maximum dose.

Beam	Energy	Beam quality
	Nominal energy	
Photon sources	(MV)	$\%dd(10)_x$
<sup>60</sup> Co Eldorado 6 <sup>a</sup>	...	58.4
Siemens KD <sup>b</sup>	6	67.0
	18	77.7
Elekta SL25 <sup>b</sup>	6	67.3
	25	82.8
Varian Clinac <sup>b</sup>	4	62.7
	6	66.5
	10	73.8
	15	77.8
	18	81.5
Varian Clinac <sup>c</sup>	24	86.1
Varian Clinac (flattening filter free) <sup>d,e</sup>	6	63.7
	10	69.9
Elekta SL25 (flattening filter free) <sup>d,e</sup>	25	81.0
	Nominal energy	
Electron sources	(MeV)	$R_{50}$
Varian Clinac 2100C <sup>f</sup>	6	2.6
	9	4.0
	12	5.2
	15	6.5
	18	7.7
Elekta SL25 <sup>g</sup>	4	1.7
	22	8.8

<sup>a</sup>Reference 24.

<sup>b</sup>Reference 25.

<sup>c</sup>Reference 26.

<sup>d</sup>Reference 27.

<sup>e</sup>Based on Ref. 27 as modified by E. S. M. Ali (private communication, 2010).

<sup>f</sup>Reference 28.

<sup>g</sup>Reference 29.

tainty of 0.2% for calculations using the BEAMnrc source simulation. The beam quality specifier is the photon component of the percent depth-dose at 10 cm depth in a  $10 \times 10$  cm<sup>2</sup> field,  $\%dd(10)_x$ . The spectra are from previous publications and are listed along with  $\%dd(10)_x$  in Table II. The simulations use XCOM photon cross sections and NIST bremsstrahlung cross-sections; all other Monte Carlo transport parameters are set to default parameters in EGSnrc. The cutoff energies and production thresholds for the calculations are 521 keV for electrons and 10 keV for photons, although calculations using cutoff energies and production thresholds of 512 (electrons) and 1 keV (photons) were performed with the IBA CC01 chamber to test the effects of a reduction by a factor of 10 and confirmed that the results are not affected.

There is interest in the variation of the response of an ionization chamber with a high-Z electrode in high-energy photon beams as these chambers are often used for relative dosimetry. To investigate this,  $P_{cel}$  is calculated for the Exra-

din A16 chamber in the unfiltered Varian Clinac 6 MV beam modeled using the same configuration as above but at depths of 1, 5, 10 and 20 cm in the water phantom.

In electron beams,  $P_{cel}$  is calculated for the chambers in Table I at the reference depth in a water phantom. For electron beams, beam quality is specified by  $R_{50}$ , the depth in water at which the absorbed dose falls to 50% of the maximum dose. The reference depth  $d_{ref}$  is related to  $R_{50}$  using  $d_{ref} = 0.6R_{50} - 0.1$  (cm). The beam is modeled as a point source with tabulated spectra collimated on the surface of a  $30 \times 30 \times 30$  cm<sup>3</sup> water phantom at an SSD of 100 cm. As recommended by TG-51, for beams with  $R_{50} \leq 8.5$  cm, the field size on the surface of the phantom is  $10 \times 10$  cm<sup>2</sup>; for beams with  $R_{50} > 8.5$  cm, the field size is  $20 \times 20$  cm<sup>2</sup>. Electron beam spectra are from the literature and are tabulated with  $R_{50}$  in Table II. Only one beam, the Elekta SL25 22 MeV, has  $R_{50} > 8.5$  cm so it is the only beam where the field size is  $20 \times 20$  cm<sup>2</sup>. Monte Carlo transport parameters and particle cutoff energies are the same as those used for calculations in photon beams.

The beam quality specifiers,  $\%dd(10)_x$  for photons and  $R_{50}$  for electrons, are determined with depth-dose curves calculated using BEAMnrc.<sup>18</sup> The water phantom is a cylinder with a radius of 20 cm and a thickness of 30 cm. The beam is modeled using tabulated spectra as a point source collimated into a  $10 \times 10$  cm<sup>2</sup> field on the surface of the water phantom at a SSD of 100 cm, as prescribed by the TG-51 protocol.<sup>1</sup> Again, for the 22 MeV beam, the field size was changed to  $20 \times 20$  cm<sup>2</sup>. In photon beams, the absorbed dose-to-water is calculated along the central axis of a cylindrical water phantom in individual disks of water with thicknesses of 0.2 cm and radii of 0.5 cm. In electron beams, the geometry is the same except that the water disks are 0.1 cm thick. The calculated  $\%dd(10)_x$  values are given in Table II and they differ by less than 0.2% from the results of Kalach and Rogers<sup>19</sup> for the beams where values are available. Similarly, calculated  $R_{50}$  values are given in Table II.

Given the large effect of high-Z central electrodes on  $k_Q$  in high-energy photon beams, there is interest in studying the effects for these ion chambers in low-energy photon beams. Two situations are investigated: central electrode effects as a function of distance from an <sup>192</sup>Ir point source in water and as a function of depth in a water phantom on which a kilovoltage x-ray beam is incident. While  $P_{cel}$  corrections are not directly used for low-energy beams, the variation of the absorbed dose sensitivity of these chambers (i.e.,  $D_{ch}^{el}/D_w$ ) is closely related to the  $P_{cel}$  variation studied here.

The central electrode effect is investigated in water as a function of distance from an iridium-192 high dose-rate brachytherapy source. The source is modeled as an isotropic point source at the midpoint of a  $50 \times 50 \times 50$  cm<sup>3</sup> water phantom using the tabulated spectrum for the <sup>192</sup>Ir Vari-Source given by Borg and Rogers.<sup>20</sup> Calculations of  $P_{cel}$  for the Exradin A16 and NE2571 ion chambers are performed between 1 and 8 cm from the point source at 1 cm intervals. Additionally, to see if the observed effects are due to the change in the Ir-192 spectrum as a function of depth in water,

the calculations are repeated for the A16 chamber, keeping all quantities the same except changing the water in the phantom to dry air. These in-air calculations are used for a comparison with the simulations in phantom so the calculations are for only two distances from the point source, 1 and 8 cm. To ensure accuracy in the simulations at these lower photon energies, electron and photon cutoff energies are set to 512 and 1 keV, respectively. Default EGSnrc Monte Carlo transport parameters are used except that XCOM photon cross-sections and NIST bremsstrahlung cross-sections are used and Rayleigh scattering is turned on.

The central electrode correction factor is calculated for ion chambers as a function of depth in a water phantom with an incident x-ray beam. The source is modeled as a point source collimated to a  $10 \times 10$  cm<sup>2</sup> field on the surface of a  $30 \times 30 \times 30$  cm<sup>3</sup> water phantom at a SSD of 52 cm. A tabulated spectrum is used to simulate the Comet MXR-320 200 kVp x-ray source as given by Mainegra-Hing and Kawarackow.<sup>21</sup> The HVL thickness for this spectrum is 1.0851 mm Cu as reported in that work.<sup>21</sup> The value of  $P_{cel}$  is calculated for the Exradin A16, A12, and NE2571 ion chambers at depths between 1 and 5 cm at 1 cm intervals. The particle cutoff energies and Monte Carlo transport parameters are the same as for the <sup>192</sup>Ir calculations.

### III. RESULTS AND DISCUSSION

#### III.A. Photon beams

Figure 1 shows  $P_{cel}$  values for ion chambers with C552 or aluminum electrodes in photon beams as a function of

$\%dd(10)_x$ . In all figures in this work, error bars represent the relative statistical uncertainty on the Monte Carlo calculations. Muir and Rogers<sup>5</sup> determined that the central electrode adds a negligible component to the systematic uncertainty in  $k_Q$  values compared to the relative statistical uncertainty of the Monte Carlo calculations so the overall uncertainty on these  $P_{cel}$  calculations is dominated by the relative statistical uncertainty. There are several notable features in Fig. 1. Calculations of  $P_{cel}$  for the Exradin A12 chamber with a C552 electrode are all within 0.1% of unity, regardless of beam filtration. Traditionally, it is assumed that the central electrode does not need to be taken into account if the electrode is composed of the same material as the wall.<sup>22</sup> This assumption was used for TG-51 calculations for the A12 chamber.<sup>1</sup> Near unity values of  $P_{cel}$  confirm the validity of the assumption for this chamber. NE2571  $P_{cel}$  calculations in beams with a flattening filter (filtered) are in good agreement with values provided by Buckley *et al.*<sup>11</sup> and TG-51  $P_{cel}$  values for a 1 mm diameter aluminum electrode.<sup>1</sup>  $P_{cel}$  calculations for the NE2571 in linear accelerator beams without a flattening filter (unfiltered) are all lower than TG-51 values by up to 0.2%. The NE2561  $P_{cel}$  calculations with a 2 mm diameter hollow aluminum electrode are all close to 0.3% lower than the NE2571 values in filtered beams. This can be explained by the larger fraction of the collecting volume occupied by the electrode in the NE2561 (6.2%, although only 2.3% is composed of aluminum) compared to 2.3% for the NE2571. The PTW 31014 employs an aluminum electrode with a smaller radius (0.09 mm) and length (4 mm) than in the NE2571. Figure 1 shows that the central electrode effect for

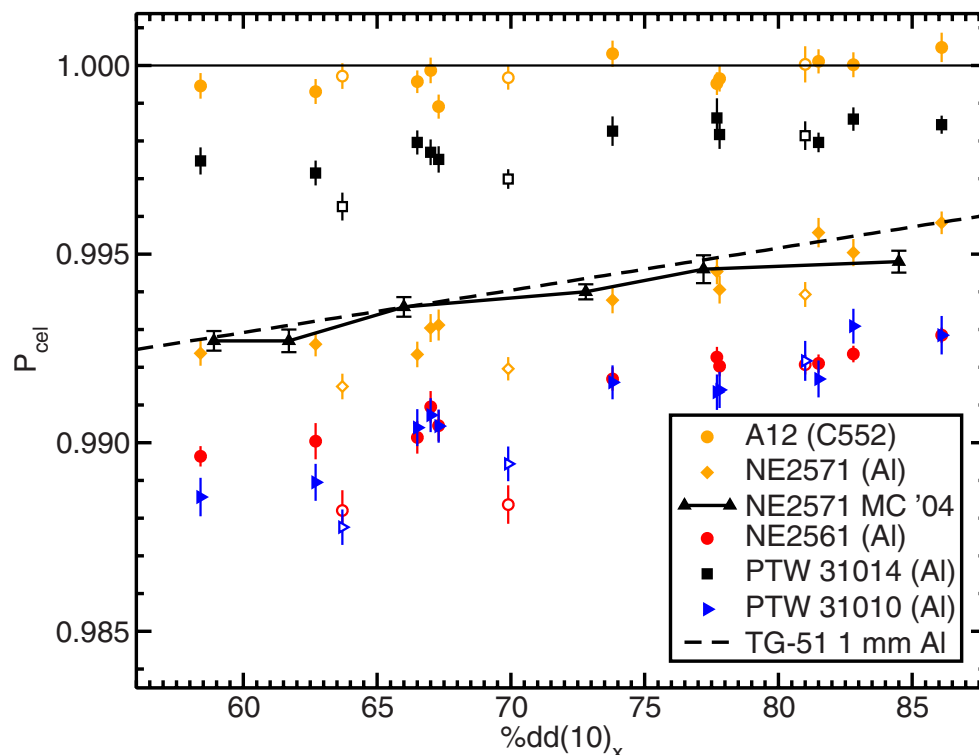


FIG. 1.  $P_{cel}$  for ion chambers in photon beams plotted against  $\%dd(10)_x$  for chambers with C552 or aluminum electrodes. Solid symbols are filtered beams and open symbols are unfiltered beams. MC '04 data are from Buckley *et al.* (Ref. 11).

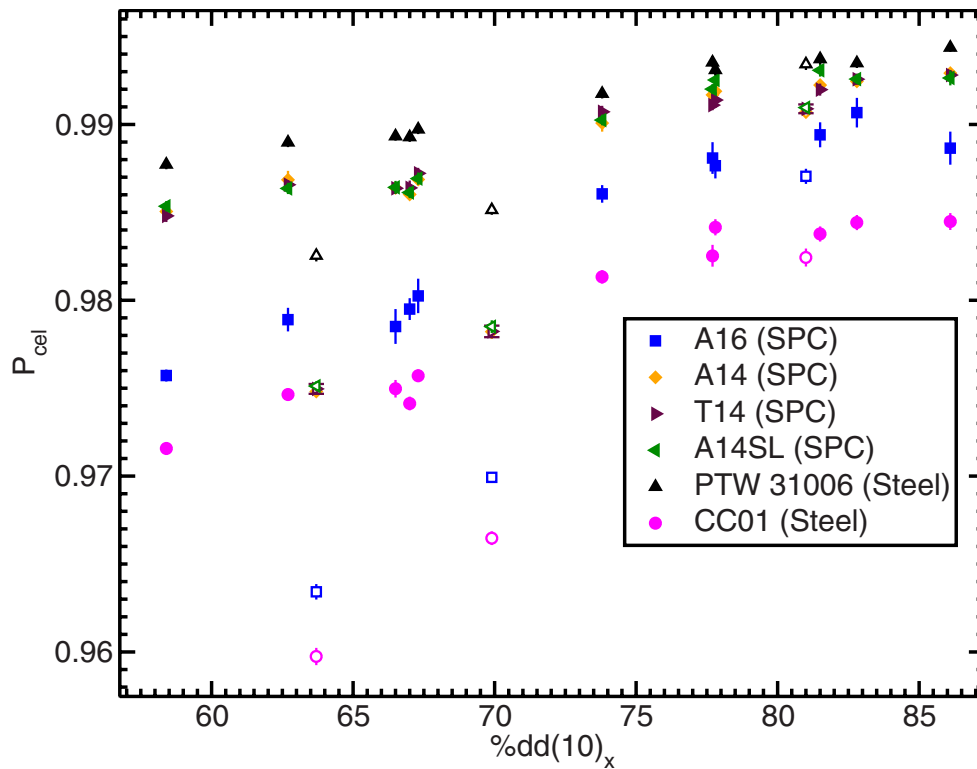


FIG. 2.  $P_{cel}$  for ion chambers in photon beams plotted against  $\%dd(10)_x$  for chambers with high-Z electrodes. Error bars are smaller than symbols if not visible. Solid symbols are filtered beams and open symbols are soft beams.

the PTW 31014 is smaller than for the NE2571 and that the deviation between  $P_{cel}$  calculations in filtered and unfiltered beams is less dramatic than for the NE2571 chamber. These characteristics are ascribed to the lower fraction of the cavity volume occupied by the electrode in the PTW 31014 chamber (0.7% vs 2.3% for the NE2571). The PTW 31010 also uses an aluminum electrode but the model given by Wulff *et al.*,<sup>23</sup> used here, has a much larger fraction of cavity volume (12.1%) occupied by the central electrode than in the NE2571 chamber. This explains the larger central electrode effect for this chamber compared to other chambers that use aluminum electrodes.

Figure 2 shows  $P_{cel}$  calculations for ion chambers with electrodes composed of materials with  $Z > 13$  in photon beams. The Exradin A16, A14, A14SL, and T14 chambers use silver-plated copper covered (SPC) steel electrodes while the IBA CC01 and PTW 31006 use steel electrodes. The high effective atomic number of these electrodes increases the probability of electrons being created, contributing to a higher dose to the smaller for ion chambers that include the higher-Z central electrode. The resulting impact on  $P_{cel}$  is seen in Fig. 2 where  $P_{cel}$  is generally much lower than for those chambers with an aluminum electrode seen in Fig. 1. The electrode occupies a larger fraction of the cavity volume in the A16 (1.0%) chamber than in the A14, A14SL, and T14 chambers (all 0.4%), explaining the larger central electrode effect for the A16 chamber. The SPC electrodes occupy the same fraction of the cavity volume in the A14, A14SL, and T14 chambers, resulting in tightly grouped  $P_{cel}$  values. The

IBA CC01 and PTW 31006 electrodes are modeled using the same material, but  $P_{cel}$  calculations differ because of the lower fraction of the cavity volume occupied by the electrode in the PTW 31006 (0.7%) than the CC01 (2.5%). There is a large difference between  $P_{cel}$  values in filtered and unfiltered beams for the same chamber in neighboring beam qualities for all chambers using high-Z electrodes. This implies that  $\%dd(10)_x$  is not an adequate beam quality specifier for these ionization chambers.  $P_{cel}$  values were also plotted as a function of calculated  $TPR_{10}^{20}$  values (not shown) but the

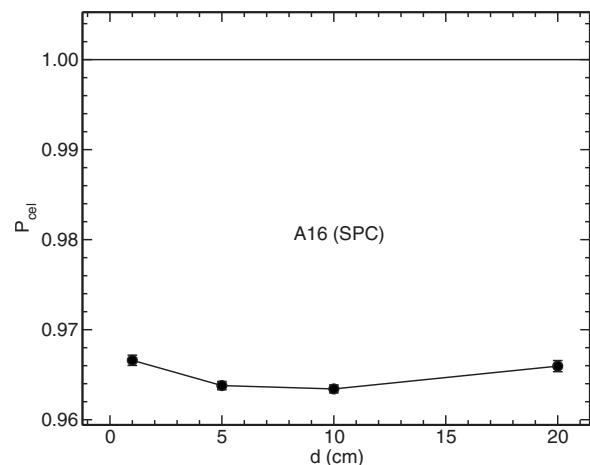


FIG. 3.  $P_{cel}$  for the Exradin A16 ion chamber as a function of depth in the unfiltered (flattening filter free) Varian Clinac 6 MV beam.

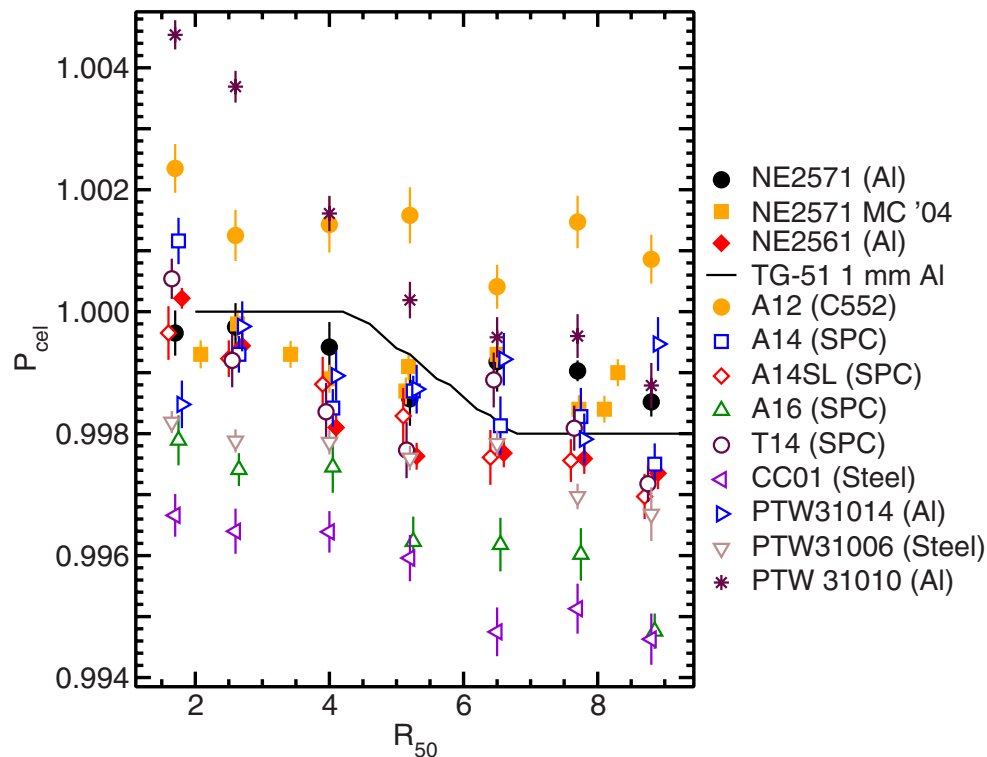


FIG. 4.  $P_{cel}$  for ion chambers in electron beams plotted against  $R_{50}$ . MC '04 data are from Buckley *et al.* (Ref. 11). Some  $R_{50}$  values have been offset for clarity; offsets are  $-0.1$ ,  $-0.05$ ,  $0.05$ ,  $0.05$ ,  $0.1$ , and  $0.1$  cm for the A14SL, T14, A14, A16, NE2561, and PTW31014 chambers, respectively.

situation did not improve, i.e.,  $TPR_{10}^{20}$  is also an inadequate beam quality specifier for these ion chambers.

Figure 3 shows that  $P_{cel}$  calculations for the Exradin A16 ion chamber vary by less than 0.35% as the depth of the chamber is varied from 1 to 20 cm in the unfiltered Varian Clinac 6 MV beam. The lack of variation is somewhat surprising given the significant variation between  $P_{cel}$  values in filtered compared to unfiltered beams.

### III.B. Electron beams

Figure 4 shows that the variation of  $P_{cel}$  values in electron beams is not as dramatic as that in photon beams. The calculated  $P_{cel}$  factors for the Exradin A12 chamber are almost all slightly larger than the previously used value of unity by up to 0.2%.  $P_{cel}$  calculations for the NE2571 chamber agree with the results of Buckley *et al.*<sup>11</sup> Calculations of  $P_{cel}$  for the NE2561 chamber with a hollow aluminum electrode are within 0.1% of the TG-51 calculations for a 1 mm diameter aluminum electrode, except for two points that are close to 0.2% low (for  $R_{50} \approx 4-5$  cm). The  $P_{cel}$  calculations for the PTW 31014 are in good agreement with TG-51 calculations, except for the highest and lowest energy data points which both differ by 0.15%. For the PTW 31010 chamber, with a much larger aluminum electrode,  $P_{cel}$  calculations are 0.45% higher than TG-51 calculations at low energies. The difference decreases with increasing beam energy. The  $P_{cel}$  calculations for the Exradin A14, A14SL, and T14 (SPC electrodes) are surprisingly close to TG-51 values for a 1 mm diameter aluminum electrode, with maximum deviations less

than 0.2%. The calculations of the central electrode correction factor for the PTW 31006 (steel electrode) in the low to mid-energy regime ( $R_{50} < 5.5$  cm) have  $P_{cel}$  factors that are all about 0.2% lower than TG-51 calculations. The Exradin A16 (SPC) and IBA CC01 (steel) chambers exhibit the worst deviations from TG-51 calculations with a 1 mm diameter aluminum electrode.  $P_{cel}$  calculations for the A16 chamber are between 0.2% and 0.3% lower than TG-51 values, while calculations for the CC01 chamber are 0.2%–0.4% lower.

### III.C. Effects on beam quality conversion factors

For dosimetry protocols, the value of  $P_{cel}$  in a beam of quality  $Q$  vs that in a  $^{60}\text{Co}$  beam is relevant for beam quality conversion factors  $k_Q$ . It is possible that the difference between calculated and TG-51  $P_{cel}$  values in photon beams is less problematic than one might expect based on the larger differences from unity for  $P_{cel}$  since the variation with respect to  $^{60}\text{Co}$  is not so dramatically different. In the worst case, for the Exradin A16 chamber, the ratio of  $P_{cel}$  in a photon beam of quality  $Q$  to that in a  $^{60}\text{Co}$  beam varies from 0.987 for an unfiltered, low-energy beam (Varian 6 MV flattening filter free) to 1.015 for a filtered, high-energy beam (Elekta SL25 25 MV), while the same ratio for the NE2571 chamber only varies from 0.9991 to 1.0027 for the same beams, respectively. However, the A16 represents a worst case for photon beams and if one ignores the flattening filter free beams, the  $(P_{cel})_Q / (P_{cel})_{^{60}\text{Co}}$  ratio varies from 1.000 to 1.008 for all of the other detectors.

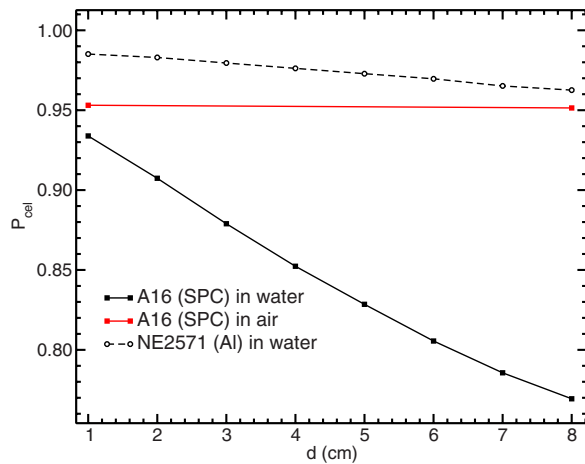


FIG. 5.  $P_{cel}$  for ion chambers as a function of distance from an  $^{192}\text{Ir}$  point source. Symbols are larger than error bars.

New values of  $P_{cel}$  for high-Z electrodes will cause a much larger change in electron beam dosimetry because of the significant values of  $P_{cel}$  in  $^{60}\text{Co}$  beams. The ratio of  $P_{cel}$  in an electron beam of quality  $Q$  to that in a  $^{60}\text{Co}$  beam for the Exradin A16 is between 1.0227 and 1.0195 for the lowest and highest energy electron beams, respectively, while for the NE2571 chamber, the ratio is between 1.0073 and 1.0062. For electron beams, there are six chambers for which this ratio exceeds 1.010 for all values of  $R_{50}$ .

### III.D. $^{192}\text{Ir}$ source

Figure 5 shows the  $P_{cel}$  results for two chambers as a function of distance from an  $^{192}\text{Ir}$  point source. For both the Exradin A16 and NE2571 chambers, the effect of the central electrode increases as the energy spectrum changes with increasing distance from the source.  $P_{cel}$  does not vary for the A16 chamber as a function of distance in air since the spectrum changes little. The average photon energy decreases by 11.5% (from 322 to 285 keV) with increasing distance from the point source in water, explaining the increased effect of the central electrode. For the A16 chamber, the effect varies by almost 17% as the distance from the source increases from 1 to 8 cm. For the NE2571, the effect is less dramatic with a variation of only 2% as distance from the source increases.

### III.E. Kilovoltage x-ray beam

Figure 6 shows results for  $P_{cel}$  for the (a) NE2571, (b) Exradin A16, and (c) Exradin A12 chambers as a function of depth in a water phantom with an incident 200 kVp beam from a point source. The results are intriguing; although the electrode effects are very large, the variation for NE2571 (Al) and the Exradin A16 (SPC) as a function of depth is much less dramatic than for the  $^{192}\text{Ir}$  case and in opposite directions from each other. The change in average photon energy on the central axis does not explain the different directions of variation. Performing calculations with the NE2571 chamber but with an SPC electrode, scaled to the

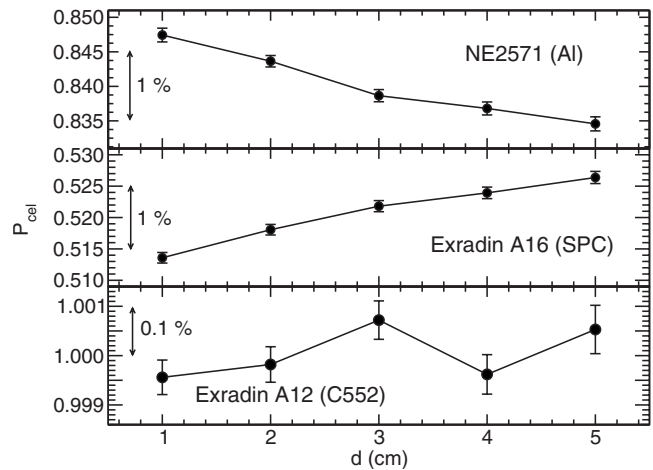


FIG. 6.  $P_{cel}$  for the NE2571, Exradin A16, and Exradin A12 ion chambers as a function of depth from the surface of a water phantom on which a 200 kVp x-ray beam is incident. The relative statistical uncertainty on Exradin A12 values is less than 0.05% even though the error bars are large on this scale.

size of the original aluminum electrode, shows variation in the same direction as calculations with an aluminum electrode. The variation must depend in a complex way on the surroundings of the electrode. The central electrode effect is on the order of 15% for the NE2571 chamber and 50% for the Exradin A16 chamber. These observations can be explained by the strong dependence of the photoelectric effect on atomic number in this low-energy range. The much higher effective atomic number of the A16 electrode results in a very large central electrode correction. However, the variation with depth is only about 2%, much less than in the  $^{192}\text{Ir}$  case. The Exradin A12 chamber with a C552 electrode does not exhibit a significant  $P_{cel}$  correction, with values within 0.1% of unity, and shows no significant variation with depth.

## IV. CONCLUSIONS

The central electrode correction factors for chambers with high-Z electrodes, which were not characterized by current dosimetry protocols,<sup>1,3,4</sup> are different from those for chambers with aluminum electrodes. The difference between  $P_{cel}$  for high-Z compared to aluminum electrodes is dramatic for photon beams but less problematic for electron beams. These results are superficially misleading since what is important for dosimetry protocols is the variation of  $P_{cel}$  compared to that in a cobalt-60 beam. In photon beams, the variation is not so dramatic although still significant. A much larger change is observed in electron beams because of the significant nonunity values of  $P_{cel}$  in cobalt-60 beams. These observations indicate that  $k_Q$  values from current dosimetry protocols should not be used for chambers with high-Z electrodes. Beam filtration also affects  $P_{cel}$  for high-Z electrodes in photon beams. Calculations of  $P_{cel}$  as a function of distance from low-energy photon sources show variation as a function of distance from the source and between chamber models.

It is important that clinical medical physicists be aware of these issues for chambers with high-Z electrodes. If possible, it would be best for manufacturers to avoid producing chambers that employ high-Z electrodes.

## ACKNOWLEDGMENTS

The authors thank Brian Hooten of Standard Imaging and Igor Gomola of IBA for ion chamber specifications and Ernesto Mainegra-Hing of NRC for the tabulated spectrum used for x-ray simulations. The authors thank E.S.M. Ali for unfiltered linear accelerator photon beam spectra and useful comments on the manuscript. This work is supported by an OGSST scholarship held by B.R. Muir, by NSERC, CRC program, CFI, and OIT.

<sup>a)</sup>Electronic mail: bmuir@physics.carleton.ca

<sup>b)</sup>Electronic mail: drogers@physics.carleton.ca

- <sup>1</sup>P. R. Almond, P. J. Biggs, B. M. Coursey, W. F. Hanson, M. S. Huq, R. Nath, and D. W. O. Rogers, "AAPM's TG-51 protocol for clinical reference dosimetry of high-energy photon and electron beams," *Med. Phys.* **26**, 1847–1870 (1999).
- <sup>2</sup>IAEA, "Absorbed dose determination in external beam radiotherapy: An international code of practice for dosimetry based on standards of absorbed dose to water," IAEA Technical Report Series No. 398 (IAEA, Vienna, 2001).
- <sup>3</sup>A. H. L. Aalbers, M. T. Hoornaert, A. Minken, H. Palmans, M. W. H. Pieksma, L. A. de Prez, N. Reynaert, S. Vynckier, and F. W. Wittkamper, "Code of practice for the absorbed dose determination in high energy photon and electron beams," NCS Report No. 18 (Netherlands Commission on Radiation Dosimetry, 2008).
- <sup>4</sup>IAEA, "Absorbed dose determination in external beam radiotherapy: An international code of practice for dosimetry based on standards of absorbed dose to water V12," IAEA Technical Report Series No. 398 (IAEA, Vienna, 2006).
- <sup>5</sup>B. R. Muir and D. W. O. Rogers, "Monte Carlo calculations of  $k_Q$ , the beam quality conversion factor," *Med. Phys.* **37**, 5939–5950 (2010).
- <sup>6</sup>M. R. McEwen, "Measurement of ionization chamber absorbed dose  $k_Q$  factors in megavoltage photon beams," *Med. Phys.* **37**, 2179–2193 (2010).
- <sup>7</sup>M. Kristensen, "Measured influence of the central electrode diameter and material on the response of a graphite ionization chamber to  $^{60}\text{Co}$  gamma-rays," *Phys. Med. Biol.* **28**, 1269–1278 (1983).
- <sup>8</sup>C.-M. Ma and A. E. Nahum, "Effect of size and composition of central electrode on the response of cylindrical ionisation chambers in high-energy photon and electron beams," *Phys. Med. Biol.* **38**, 267–290 (1993).
- <sup>9</sup>A. Palm and O. Mattsson, "Experimental study on the influence of the central electrode in Farmer-type ionization chambers," *Phys. Med. Biol.* **44**, 1299–1308 (1999).
- <sup>10</sup>F. Ubrich, J. Wulff, R. Kranzer, and K. Zink, "Thimble ionization chambers in medium-energy x-ray beams and the role of constructive details of the central electrode: Monte Carlo simulations and measurements," *Phys. Med. Biol.* **53**, 4893–4906 (2008).

- <sup>11</sup>L. A. Buckley, I. Kawrakow, and D. W. O. Rogers, "CSnrc: Correlated sampling Monte Carlo calculations using EGSnrc," *Med. Phys.* **31**, 3425–3435 (2004).
- <sup>12</sup>F. Tessier and I. Kawrakow, "Effective point of measurement of thimble ion chambers in megavoltage photon beams," *Med. Phys.* **37**, 96–107 (2010).
- <sup>13</sup>T. Shimono, K. Kochida, H. Nambu, K. Matsubara, H. Takahashi, and H. Okuda, "Polarity effect in commercial ionization chambers used in photon beams with small fields," *Radiol. Phys. Technol.* **2**, 97–103 (2009).
- <sup>14</sup>R. Hill, Z. Mo, M. Haque, and C. Baldock, "An evaluation of ionization chambers for the relative dosimetry of kilovoltage x-ray beams," *Med. Phys.* **36**, 3971–3981 (2009).
- <sup>15</sup>F. Crop, N. Reynaert, G. Pittomvils, L. Paelinck, C. D. Wagter, L. Vakaet, and H. Thierens, "The influence of small field sizes, penumbra, spot size and measurement depth on perturbation factors for microionization chambers," *Phys. Med. Biol.* **54**, 2951–2969 (2009).
- <sup>16</sup>J. Wulff, K. Zink, and I. Kawrakow, "Efficiency improvements for ion chamber calculations in high energy photon beams," *Med. Phys.* **35**, 1328–1336 (2008).
- <sup>17</sup>I. Kawrakow, "Accurate condensed history Monte Carlo simulation of electron transport. II. Application to ion chamber response simulations," *Med. Phys.* **27**, 499–513 (2000).
- <sup>18</sup>D. W. O. Rogers, B. Walters, and I. Kawrakow, "BEAMnrc users manual," NRC Report No. PIRS 509(a), Rev. K, 2006.
- <sup>19</sup>N. I. Kalach and D. W. O. Rogers, "Which accelerator photon beams are 'clinic-like' for reference dosimetry purposes?," *Med. Phys.* **30**, 1546–1555 (2003).
- <sup>20</sup>J. Borg and D. W. O. Rogers, "Spectra and air-kerma strength for encapsulated  $^{192}\text{Ir}$  sources," *Med. Phys.* **26**, 2441–2444 (1999).
- <sup>21</sup>E. Mainegra-Hing and I. Kawrakow, "Efficient x-ray tube simulations," *Med. Phys.* **33**, 2683–2690 (2006).
- <sup>22</sup>D. W. O. Rogers, in *Clinical Dosimetry Measurements in Radiotherapy*, edited by D. W. O. Rogers and J. E. Cygler (Medical Physics, Madison, 2009), pp. 239–296.
- <sup>23</sup>J. Wulff, J. T. Heverhagen, and K. Zink, "Monte-Carlo-based perturbation and beam quality correction factors for thimble ionization chambers in high-energy photon beams," *Phys. Med. Biol.* **53**, 2823–2836 (2008).
- <sup>24</sup>G. Mora, A. Maio, and D. W. O. Rogers, "Monte Carlo simulation of a typical  $^{60}\text{Co}$  therapy source," *Med. Phys.* **26**, 2494–2502 (1999).
- <sup>25</sup>D. Sheikh-Bagheri and D. W. O. Rogers, "Monte Carlo calculation of nine megavoltage photon beam spectra using the BEAM code," *Med. Phys.* **29**, 391–402 (2002).
- <sup>26</sup>R. Mohan, C. Chui, and L. Lidofsky, "Energy and angular distributions of photons from medical linear accelerators," *Med. Phys.* **12**, 592–597 (1985).
- <sup>27</sup>G. Xiong and D. W. O. Rogers, "Relationship between  $\%dd(10)_x$  and stopping-power ratios for flattening filter free accelerators: A Monte Carlo study," *Med. Phys.* **35**, 2104–2109 (2008).
- <sup>28</sup>G. X. Ding and D. W. O. Rogers, "Energy spectra, angular spread, and dose distributions of electron beams from various accelerators used in radiotherapy," NRC Report No. PIRS-0439 (NRC, Ottawa, 1995).
- <sup>29</sup>L. L. W. Wang and D. W. O. Rogers, "Replacement correction factors for cylindrical ion chambers in electron beams," *Med. Phys.* **36**, 4600–4608 (2009).